

Supporting Information

NosA Catalyzing Carboxyl-Terminal Amide Formation in Nosiheptide Maturation via Enamine Dealkylation on the Serine-Extended Precursor Peptide

Yi Yu, Heng Guo, Qi Zhang, Lian Duan, Ying Ding, Rijing Liao, Chun Lei, Ben Shen, and Wen Liu*

State Key Laboratory of Bioorganic and Natural Products Chemistry, Shanghai Institute of Organic Chemistry, Chinese Academy of Sciences, 345 Lingling Rd., Shanghai 200032, China; and Division of Pharmaceutical Sciences, School of Pharmacy, University of Wisconsin-Madison 777 Highland Ave., Madison WI 53705, USA

Corresponding author for Wen Liu, Tel: (+86)21-54925111, Fax: (+ 86) 21-64166128, and

E-mail: wliu@mail.sioc.ac.cn

Table of Contents

1. Experimental Section

- 1.1. Bacterial strains, plasmids, and reagents
- 1.2. DNA isolation, manipulation, and sequencing
- 1.3. Inactivation of *nosA* in *S. actuosus* ATCC 25421
- 1.4. In trans expression of *nosA* for homologous complementation
- 1.5. In trans expression of *nocA* for heterologous complementation
- 1.6. Production and analysis of nosiheptide and the intermediate **2**
- 1.7. Isolation and purification of the intermediate **2**
- 1.8. Structural elucidation of the intermediate **2**
- 1.9. Expression, purification and analysis of NosA
- 1.10. Characterization of NosA-catalyzed reaction in vitro
- 1.11. Stability of the intermediate **2** in the buffer varying in pH
- 1.12. NosA-catalyzed conversion of **X** to **Y**
- 1.13. Optimization of NosA-catalyzed reaction
- 1.14. Kinetic analysis for NosA-catalyzed reaction
- 1.15. Minimum inhibitory concentration (MICs) of nosiheptide and the intermediate **2**
- 1.16. Sequence analysis of NosA

2. Supplementary Tables

Table S1. Bacterial strains and plasmids used in this study

Table S2. Minimum inhibitory concentration (MICs) of **1** and the intermediate **2**

3. Supplementary Figures

- Figure S1. MS/MS spectrum for the intermediate **2**
- Figure S2. HR-ESI-MS and MS/MS analyses of the intermediate **2**
- Figure S3. NMR spectra of the intermediate **2** for structural elucidation
- Figure S4. Sequence comparison
- Figure S5. Structures of nosiheptide, nocathiacin I, GE2270A, thiostrepton, and siomycin A
- Figure S6. Analysis of the purified NosA
- Figure S7. Identification of the co-product pyruvate (**3**) in NosA-catalyzed reaction
- Figure S8. Effect of pH on the stability of the intermediate **2**
- Figure S9. Time dependence for converting the intermediate **2** to the hydrolyzed product **X**
- Figure S10. Sulfhydryl derivatization by adding of 5,5'-dithio-bis(2-nitrobenzoic acid) (DTNB)
- Figure S11. HR-ESI-MS and MS/MS analyses of compound **X** and its structural prediction
- Figure S12. HR-ESI-MS and MS/MS analyses of compound **Y** and its structural prediction
- Figure S13. Effect of pH on the activity of NosA
- Figure S14. Kinetic characterization of NosA by plotting the initial velocities of **1** production

1. Experimental Section

1.1. Bacterial strains, plasmids, and reagents

Bacterial strains and plasmids used in this study are summarized in Table S1. Biochemicals and media were purchased from Sinopharm Chemical Reagent Co., Ltd. (Shanghai, China) and Oxoid Ltd. (Basingstoke, United Kingdom) unless otherwise stated. Restriction enzymes were purchased from TaKaRa Biotechnology (Dalian) Co., Ltd. (Dalian, China).

1.2. DNA isolation, manipulation, and sequencing

DNA isolation and manipulation in *Escherichia coli* and *Streptomyces* were performed according to standard methods.^{1,2} PCR amplifications were carried out on an authorized thermal cycler (Eppendorf AG 22331, Hamburg, Germany) using *LA Taq* DNA polymerase (TaKaRa). Primer synthesis and DNA sequencing were performed at Shanghai Invitrogen Biotech Co., Ltd. (China).

1.3. Inactivation of *nosA* in *S. actuosus* ATCC 25421

To inactivate *nosA*, the cosmid pSL4001 serves as the template for PCR amplification.³ The 1.9 kb fragment obtained by using the primers 5'-AAG CTT GAA CTG GTC TCC ACG GTC ATC CTG C-3' (HindIII site underlined) and 5'-T CTA GAC CAC AGG ACG ACC GTG CAG TAC AGC-3' (XbaI site underlined) and a 1.9 kb fragment obtained by using the primers 5'-TCT AGA CCG GGC GCC GAC GCC TTC ATC CCC-3' (XbaI site underlined) and 5'-ATG AAT TCG ACG TCG TAC ATC TCG CCC TTG GTC-3' (EcoRI site underlined) were initially cloned into pMD19-T, giving pSL4030 and pSL4031, respectively. After sequencing to confirm the fidelity,

the 1.9 kb HindIII/XbaI and 1.9 kb XbaI/EcoRI fragments were recovered and co-ligated into the HindIII/EcoRI site of pKC1139, yielding the recombinant plasmid pSL4032, in which a 366 bp in-frame coding region (corresponding to AA₁₇-AA₁₃₈ of the deduced product NosA) of *nosA* was deleted.

Introduction of pSL4032 into *S. actuosus* was carried out by *E. coli*-*Streptomyces* conjugation, following the procedure described previously.³ The colonies that were apramycin-resistant at 37°C were identified as the integrating mutants, in which a single-crossover homologous recombination event took place. These mutants were further cultured in liquid TSB medium for three rounds in the absence of apramycin. The genotypes of resulting strains that were apramycin-sensitive were confirmed by PCR amplification and sequencing, leading to the identification of the recombinant strain SL4008.

1.4. In trans expression of *nosA* for homologous complementation

To make *nosA* expression construct, a 0.55 kb *nosA*-containing fragment was amplified from the cosmid pSL4001³ by PCR using the primers 5'-A AGC TTG AGT TCA CCG CGA ACC TCT TCC ACC-3' (HindIII site underlined) and 5'-TC TAG ACC GCG GAA GGC GCT GAT TTT TGG TGG-3' (XbaI site underlined). After digestion with HindIII and XbaI, this PCR product was ligated with a 0.45 kb EcoRI/HindIII fragment into the EcoRI/XbaI site of pSET152, yielding the recombinant plasmid pSL4034, in which *nosA* is under the control of the *PermE** promoter. Introduction of pSL4034 into SL4008 (*nosA* mutant), generating the corresponding recombinant strain SL4010 for *nosA*-expressing.

1.5. In trans expression of *nocA* for heterologous complementation

To make *nocA* expression construct, a 1.1 kb *nocA*-containing fragment was amplified from the cosmid pSL5001⁴ by PCR using the primers 5'-GCC AAG CTT GAC GCC GCC GTG GCC AGG AGG ACG-3' (HindIII site underlined) and 5'-C AGT CTA GAC GGC GCG ATG TCG GCT CCG GTG-3' (XbaI site underlined). After digestion with HindIII and XbaI, this PCR product was ligated with a 0.45 kb EcoRI/HindIII fragment into the EcoRI/XbaI site of pSET152, yielding the recombinant plasmid pSL4033, in which *nocA* is under the control of the *Perme** promoter. Introduction of pSL4033 into SL4008 (*nosA* mutant), generating the corresponding recombinant strain SL4009 for *nocA*-expressing.

1.6. Production and analysis of nosiheptide and the intermediate 2

The *S. actuosus* strains were grown on ISP2 agar plates at 30°C for sporulation. For production, 50 µl of *S. actuosus* spores were inoculated into a 250-ml flask containing 50 ml of seed medium (sucrose 2.0%, corn steep liquor 3.0%, peptone 0.5% and CaCO₃ 0.5%) and incubated at 28°C and 250 rpm for 24 hrs. Ten ml of seed culture was then transferred into 100 ml of fermentation medium (Pharmamedia cotton meal 1.0%, NaCl 0.3%, glucose 3.0%, 2 x trace elements solution 0.5% and CaCO₃ 0.3%, pH 7.0) in a 500-ml flask and incubated at 28°C for 4 days.

Each 100 ml of culture broth was centrifuged for 10 min at 6,000 rpm. After removing the supernatant, the precipitate was soaked with 100 ml of ethyl acetate for 6 hrs. The extract was concentrated in vacuum and resolved in 1 ml of methanol for further analysis. HPLC analysis was

carried out on an Agela Promosil C18 column (4.6 × 150 mm, Cat. No.: PM952505-0, P9510525BJ0373), which was equilibrated with 60% solvent A (H₂O containing 0.1% formic acid) and 40% B (CH₃CN containing 0.1% formic acid), and developed with the following program: 0 to 4 min, constant 60% A/40% B; 4 to 10 min, a linear gradient from 60% A/40% B to 40% A/60% B; 10 to 18 min, constant 40% A/60% B; and 18 to 20 min, a linear gradient from 40% A/60% B to 60% A/40% B. This was carried out at a flow rate of 1 ml min⁻¹ and UV detection at 330 nm using an Agilent 1100 HPLC system (Agilent Technologies). Mass spectrometry (MS) and tandem MS analyses were performed on a LCQ Fleet electrospray ionization (ESI) mass spectrometer (Thermo Fisher Scientific Inc.).

1.7. Isolation and purification of the intermediate 2

Isolation of the intermediate **2** from 40 L of the SL4008 culture broth were carried out according to the method described previously for thiocillin I.⁵ For further purification, the target fraction collected by silica chromatography was evaporated in vacuum and then dissolved in chloroform/methanol (1 : 1), followed by precipitation with hexane to give the powder in yellowish color (40 mg).

1.8. Structural elucidation of the intermediate 2

Tandem Mass Spectrometry analysis was performed on a LCQ Fleet Ion Trap MSⁿ tandem mass spectrometer (Thermo Fisher Scientific Inc.). High resolution tandem MS analysis of was performed on a LTQ Orbitrap XL ETD mass spectrometer (Thermo Fisher Scientific Inc.) at the

Center of Proteome Analysis, Fudan University (Shanghai, China). NMR spectra were taken on a Bruker DRX-500 NMR spectrometer (Bruker Co., Ltd.). ¹H NMR (500MHz, d₆-DMSO) δ 11.38 (br, s, 1H), 10.39 (s, 1H), 9.54 (s, 1H), 9.42 (s, 1H), 8.63 (s, 1H), 8.60 (s, 1H), 8.47 (s, 1H), 8.31 (s, 1H), 8.17 (s, 1H), 7.84 (s, 1H), 7.81 (s, 1H), 7.79 (s, 1H), 7.69 (s, 1H), 7.56 (s, 1H), 7.28 (t, 1H, J = 7.25 Hz), 7.13 (d, 1H, J = 7.00 Hz), 6.46 (q, 1H, J = 7.00 Hz), 6.10 (s, 1H), 6.06 (s, 1H), 5.88 (s, 1H), 5.70 (s, 1H), 5.61 (s, 1H), 5.58 (s, 1H), 5.55 (s, 1H), 4.58 (br, s, 1H), 4.09 (d, 1H, J = 12.00 Hz), 3.85 (d, 1H, J = 9.50 Hz), 1.72 (d, 3H, J = 6.5 Hz); ¹³C NMR (125 MHz, d₆-DMSO) δ 181.98, 172.96, 169.92, 168.72, 168.18, 167.50, 166.33, 165.12, 164.55, 161.33, 160.01, 159.85, 159.71, 157.92, 153.36, 149.82, 149.11, 148.87, 147.74, 137.67, 136.48, 135.73, 137.30, 130.69, 130.09, 129.47, 128.83, 127.93, 127.10, 126.11, 125.56, 124.97, 124.89, 124.73, 123.42, 119.71, 118.49, 114.50, 107.74, 101.88, 66.90, 66.47, 66, 10, 56.71, 48.96, 45.12, 37.45, 29.75, 18.71, 13.68, 12.62; HR-ESI-MS m/z [M + Na]⁺ 1314.1467 (calcd for C₅₄H₄₅N₁₃O₁₄S₆Na, 1314.1431); UV/Vis λ_{max} 218 nm and 348 nm.

1.9. Expression, purification and analysis of NosA

To express NosA, a 0.5 kb DNA fragment was amplified by PCR using the primers 5'- GG AAT TCC ATA TGA CCG AAC ACC CCG CAC AGC AGC-3' (NdeI site underlined) and 5'- CC GCT CGA GCT ACG CCG GCG GCC GGG AGG-3' (XhoI site underlined) with the cosmid pSL4001 as the template. The NdeI/XhoI-digested PCR product was then ligated into the pET28a vector, giving the recombinant construct pSL4029. The fidelity of NosA in the plasmid pSL4029 was confirmed by DNA sequencing.

The construct pSL4029 was introduced into *E. coli* BL21(DE3) for NosA production. Cells were grown in the LB medium supplemented with 50 µg/mL of kanamycin at 37°C and 250 rpm until the cell density reached 0.5-0.6 at OD₆₀₀. To induce protein expression, isopropyl-β-D thiogalactopyranoside (IPTG, 0.5 mM) was added into the culture, which was further incubated at 18°C for 24 hrs.

Cells were harvested, re-suspended in the lysis buffer (50 mM phosphate, 10 mM imidazole and 300 mM NaCl, pH 8.0), and then stored at -80°C until use. After sonication (8 × 10 sec pulsed cycle), the soluble fraction of the produced protein was loaded onto a Ni-NTA resin (Qiagen, Valencia, CA) column for affinity purification. The purified protein fraction was then dialyzed in TSG buffer (50 mM Tris-HCl, 25mM NaCl, 10% glycerol and 0.02% NaN₃, pH 8.0) overnight at 4°C. Finally, the resulting NosA protein was concentrated and stored at -80 °C for in vitro assays.

For MS analysis, the purified NosA protein was subjected to matrix-assisted laser desorption ionization-time-of-flight mass spectrometry (MALDI-TOF MS) (AutoFlex MALDI-TOF-MS; Bruker Daltonics Inc.) analysis at the Research Center of Proteome Analysis, Chinese Academy of Sciences (Shanghai, China).

1.10. Characterization of NosA-catalyzed reaction in vitro

For assaying the NosA activity, 20 µL of the reaction mixture initially contained 100 µM **2** and 10 µM NosA in 50 mM sodium phosphate buffer (pH 7.5). After that 20 µL of the reaction mixture then contained 60 µM **2** and 50 nM NosA in 50 mM Tris-HCl buffer (pH 8.0). The reactions were

initiated by the addition of NosA followed by incubation at 30°C for 30 mins. To quench the reaction, 50 µl of methanol was added. NosA that was boiled at 100 °C for 10 mins was used in the control reaction.

To determine **1** production, the samples were concentrated and dissolved in 15 µl of methanol. HPLC analysis was carried out under the condition as described above. The identity of **1** was confirmed by HPLC-ESI-MS analysis (for HPLC, Agilent 1100 used; and for ESI-MS, Thermo Fisher LTQ Fleet used) under the same conditions. **1** showed an $[M + H]^+$ ion at m/z 1222.13, consistent with the molecular formula $C_{51}H_{43}N_{13}O_{12}S_6$ (1221.15 calculated).

To probe pyruvate (**3**) production, the fractions with the retention time between 0.0 to 5.0 min under the above HPLC analysis condition were collected and concentrated to dryness. The resulting samples were dissolved with 2 N HCl and incubated with 2,4-dinitrophenylhydrazine at 37°C for 10 mins. HPLC analysis was carried out on an Agilent ZORBAX SB-C18 column, which was equilibrated with 55% solvent A (H_2O containing 0.1% TFA) and 45% B (CH_3CN containing 0.1% TFA), and developed with the constant program (0 to 15 min, 55% A/45% B) at a flow rate of 1 ml min^{-1} and UV detection at 265 nm. HR-ESI-MS analysis for the resulting derivative 2-(2,4-dinitrophenylhydrazono)-propanoic acid was performed on an APEXIII 7.0 TESLA FTMS mass spectrometer (Bruker Daltonics, Inc.), showing a $[M - H]^-$ ion at $m/z = 267.0375$ (calcd for $C_9H_7N_4O_6$, 267.04).

1.11. Stability of the intermediate **2 in the buffer varying in pH**

Each 20 μL of the solution contained 60 μM **2** in 50 mM sodium acetate (pH 3.0-5.0), 50 mM sodium phosphate (pH 6.0-7.0), or 50 mM Tris-HCl (pH 8.0-9.0) buffer. The solutions with the pH at 3.0, 4.0, 5.0, 6.0, 7.0, 8.0, and 9.0, were incubated at 30°C for 17 hrs before product examination by HPLC-MS.

To evaluate the time-dependent manner for converting **2** to the hydrolyzed product **X** at pH 9.0, 20 μL of the solution containing 60 μM **2** in 50 mM Tris-HCl (pH 9.0) buffer was incubated at 30°C, and then terminated by immediately storing at -80°C at 0 min, 30 min, 1 hr, 2 hr, 12 hr, or 17 hr, before product examination by HPLC-MS. For characterizing **X** by sulfhydryl derivatization with 5,5'-dithio-bis(2-nitrobenzoic acid) (DTNB), 5 μL of DTNB stock solution (containing 2 mM DTNB and 50 mM sodium acetate in H_2O) was diluted by adding 10 μL of Tris-HCl buffer (1 M, pH 8.0) and 45 μL of water, and then mixed with 40 μL of the above 12 hr-incubated solution. After incubation at 37°C for 30 min, the reaction mixture was subjected to HPLC-MS analysis.

1.12. NosA-catalyzed conversion of X to Y

The solution containing 60 μM **2** in 50 mM Tris-HCl (pH 9.0) buffer was incubated at 30°C for 12 hrs to generate **X** before the addition of NosA (50 nM). The NosA-containing reaction mixture was further incubated at 30°C for 30 mins, and then subjected to HPLC-MS analysis. For characterizing **Y** by sulfhydryl derivatization with DTNB, the workups were identical to those for **X** described above.

1.13. Optimization of NosA-catalyzed reaction

To determine the pH dependence, 20 μL of the reaction mixture contained 50 nM NosA and 100 μM **2** in 50 mM sodium acetate (pH 4.0-5.5), 50 mM sodium phosphate (pH 6.0-7.5), or 50 mM Tris-HCl (pH 8.0-9.0) buffer. Each reaction was initiated by the addition of NosA, and then incubated at 30°C for 10 min. The workups and HPLC analyses of the reaction mixtures were identical to those noted above.

To investigate the metal ion dependence, the reactions were performed in each 50 mM Tris-HCl (20 μL , pH 8.0) buffer that contains 50 nM NosA and 100 μM **2** as described above, in the absence of EDTA, or in the presence of EDTA (1 mM and 5 mM, respectively). The workups and HPLC analyses of the reaction mixtures were identical to those noted above.

1.14. Kinetic analysis for NosA-catalyzed reaction

A time course was carried out to determine the initial rate conditions in 50 mM Tris-HCl (20 μL , pH 8.0) buffer that contains 10 nM or 50 nM NosA and 200 μM **2**. All assays were performed in duplicate. The reactions were initiated by the addition of NosA, incubated at 30°C, and then terminated by 50 μL of methanol at 2, 5, 10, 15, 30, 60, 120, and 240 min, respectively. The samples were subjected to the same workups and HPLC analysis as described above. The production of **1**, linear with respect to time during 0-10 min, was fitted into a linear equation to obtain the initial velocity.

To determine the kinetic parameters for the conversion of **2** to **1**, the reactions were carried out at 30°C for 5 min in each 20 μL of the mixture that contained 10 nM NosA, 50 mM sodium

phosphate (pH 8.0), and the substrate **2** varying at 50, 100, 150, 200, 250, and 500 μM , respectively. All assays were performed in duplicate. Each conversion was analyzed by HPLC as described above. The resulting initial velocities were then fitted to the Michaelis-Menten equation using Origin software (OriginLab, Northampton, MA) to extract K_m and K_{cat} parameters.

1.15. Minimum inhibitory concentrations (MICs) of nosiheptide and the intermediate 2

The MICs were measured by broth dilution similar to the method described previously.⁸ Each test compound was dissolved in THF to produce a stock solution (10 $\mu\text{g/ml}$), which was serially diluted into 50 μl Mueller-Hinton broth (Qingdao Hope Bio-Technology Co. Ltd., China) in a 96-well microtiter plate to a final concentration ranging from 0.0256 to 0 $\mu\text{g/ml}$. 50 μl of the test strain (10^7 - 10^8 cfu/ml, calculated according to the 0.5 McFarland standard⁹) was then added into each well of the microtiter plate. After incubation at 37°C for 18-24 hr, The MIC was determined to be the lowest concentration of compound that inhibited visible bacterial growth. All testings were carried out in duplicate.

1.16. Sequence analysis of NosA

The open reading frame for *nosA* was deduced from the sequence by performing FramePlot 4.0beta program (<http://nocardia.nih.go.jp/fp4/>). The corresponding deduced protein NosA was compared with other known proteins in the databases by available BLAST methods (<http://www.ncbi.nlm.nih.gov/blast/>). Amino acid sequence alignment was performed by the CLUSTALW method, and the DRAWTREE and DRAWGRAM methods, respectively, from

BIOLOGYWORKBENCH 3.2 software (<http://workbench.sdsc.edu>).

2. Supplementary Tables

Table S1. Bacterial strains and plasmids used in this study

Strain/Plasmid	Characteristic(s)	Reference
<i>E. coli</i>		
DH5 α	Host for general cloning	Invitrogen
BL21(DE3)	Host for protein expression	Novagen
ET12567/pUZ8002	Donor strain for conjugation between <i>E.coli</i> and	1
<i>Streptomyces</i>		
<i>Streptomyces actuosus</i>		
ATCC 25421	Wild type strain, nosiheptide (1) producing	ATCC, gift from H. G. Floss
SL4008	<i>nosA</i> mutant, intermediate 2 producing	This study
SL4009	SL4008 derivative that contains pSL4033 for expressing <i>nocA</i> in trans, 1 producing	This study
SL4010	SL4008 derivative that contains pSL4034 for expressing <i>nosA</i> in trans, 1 producing	This study
Plasmids		
pMD19-T	<i>E. coli</i> subcloning vector	TaKaRa
pET28a	Protein expression vector in <i>E. coli</i> BL21(DE3)	Novagen

pKC1139	<i>E.coli-Streptomyces</i> shuttle vector for gene 6 inactivation, temperature sensitive replication in <i>Streptomyces</i>	
pSL4001	pOJ446-based <i>S. actuosus</i> genomic library cosmid, containing the entire 1 biosynthesis gene cluster	7
pSL4029	pET28a derivative containing a 0.5 kb fragment, construct for NosA expression	This study
pSL4030	pMD19-T derivative containing a 1.9 kb PCR product from pSL4001	This study
pSL4031	pMD19-T derivative containing a 1.9 kb PCR product from pSL4001	This study
pSL4032	pKC1139 derivative containing a 3.8 kb fragment, construct for <i>nosA</i> in-frame inactivation	This study
pSL4033	pSET152 derivative containing a 1.1 kb fragment, construct for expressing <i>nocA</i> in SL4008	This study
pSL4034	pSET152 derivative containing a 0.55 kb fragment, construct for expressing <i>nosA</i> in SL4008	This study

Table S2. Minimum inhibitory concentrations (MICs) of **1** and the intermediate **2**.

Organism	Number ^a	MIC (µg/ml)	
		1	2
<i>Bacillus subtilis</i>	SIPI-JD1001	0.008	0.008

^a The test organism was deposited at Shanghai Institute of Pharmaceutical Industry (SIPI) with the given numbers.

3. Supplementary Figures

Figure S1. MS/MS spectrum for the intermediate **2** (calculated 1290.15), showing the parent [M - H]⁻ ion at $m/z = 1289.60$ and its fragments.

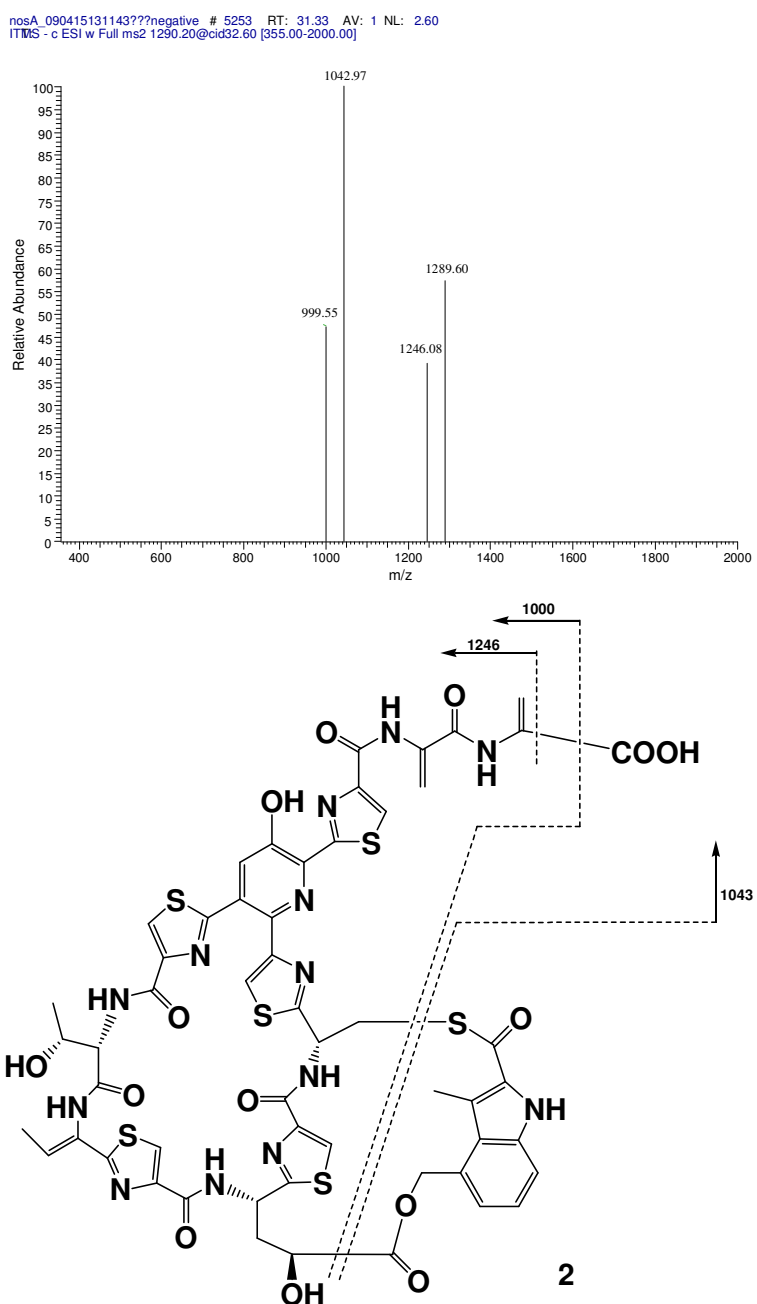
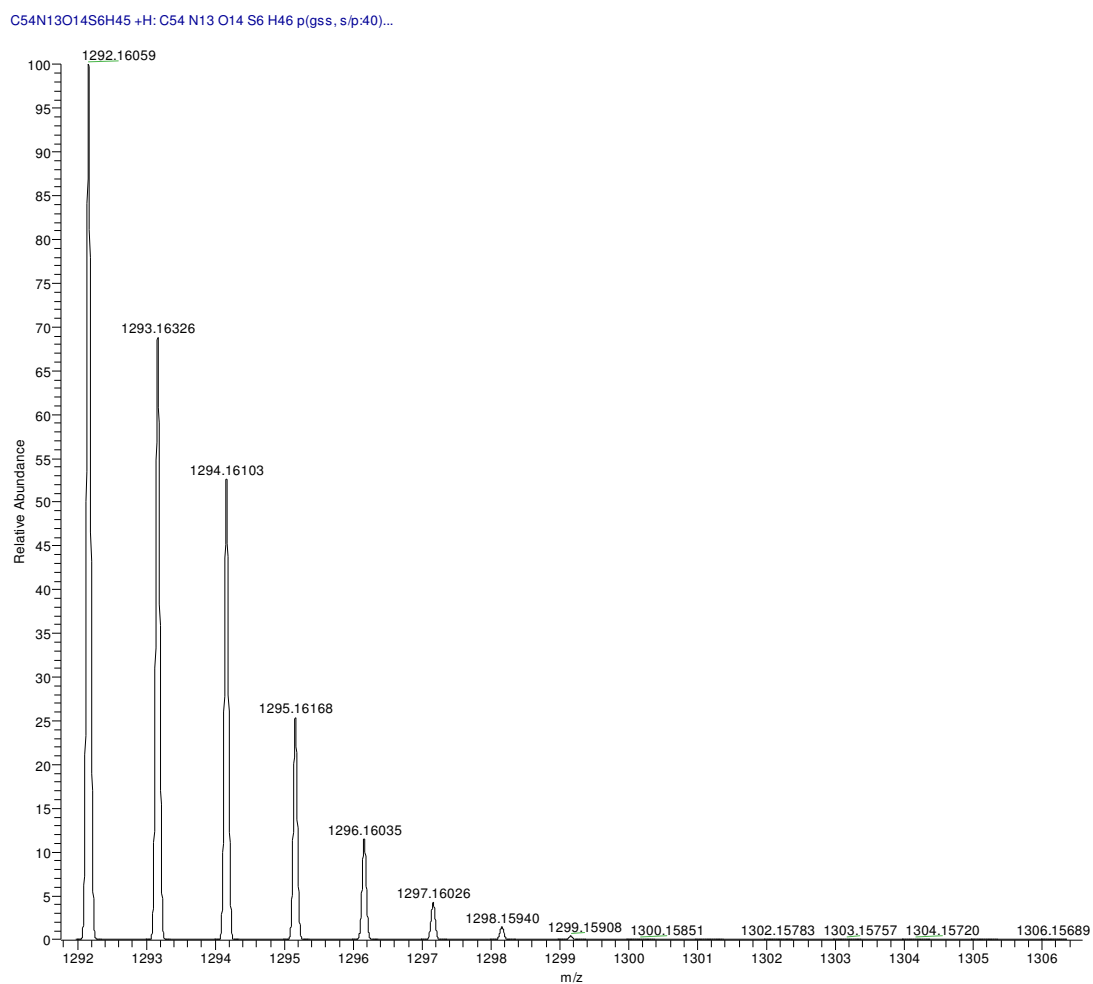


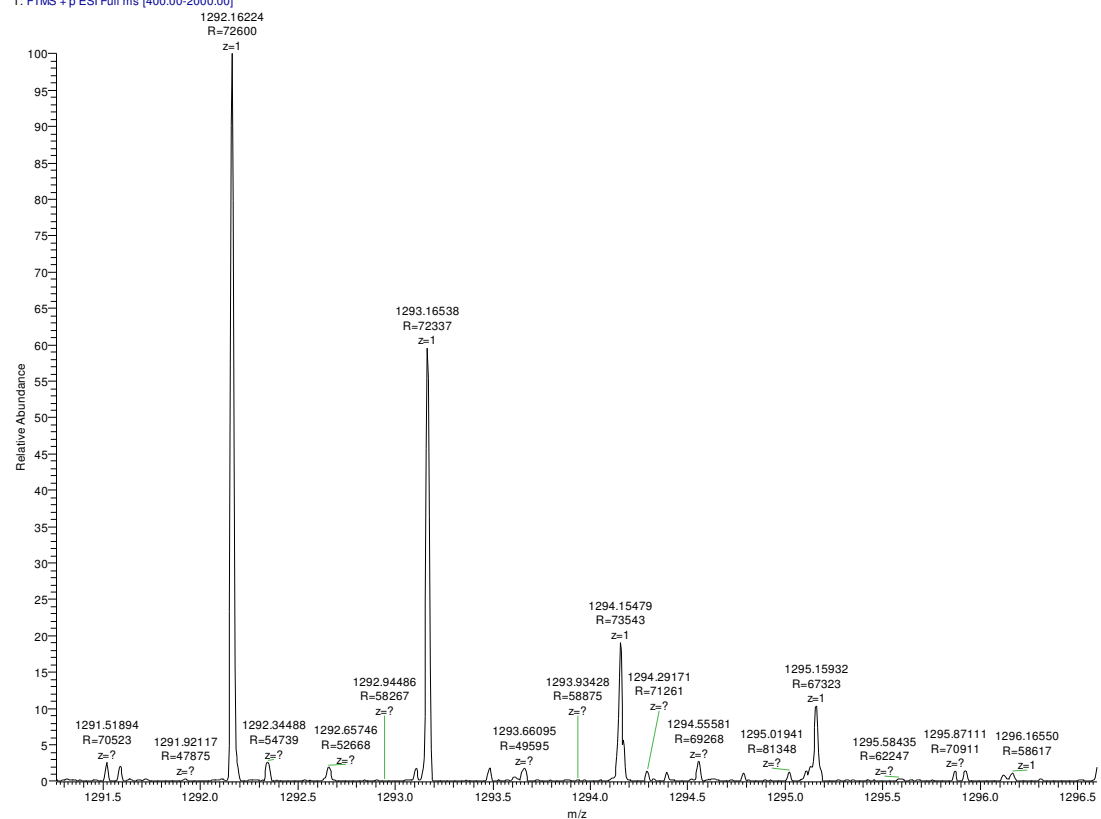
Figure S2. HR-ESI-MS and MS/MS analyses of the intermediate **2**. A, theoretical profile for the $[M + H]^+$ ion of **2** (molecular formula as $C_{54}N_{13}O_{14}S_6H_{46}^+$, calculated 1292.16059); B, obtained profile for the $[M + H]^+$ ion of **2** by Orbitrap scanning with the resolution at 100,000 ($m/z = 400$); and C, MS/MS analysis of the parent ion at $m/z = 1292.16$ corresponding to **2** by LTQ scanning and its fragments.

A



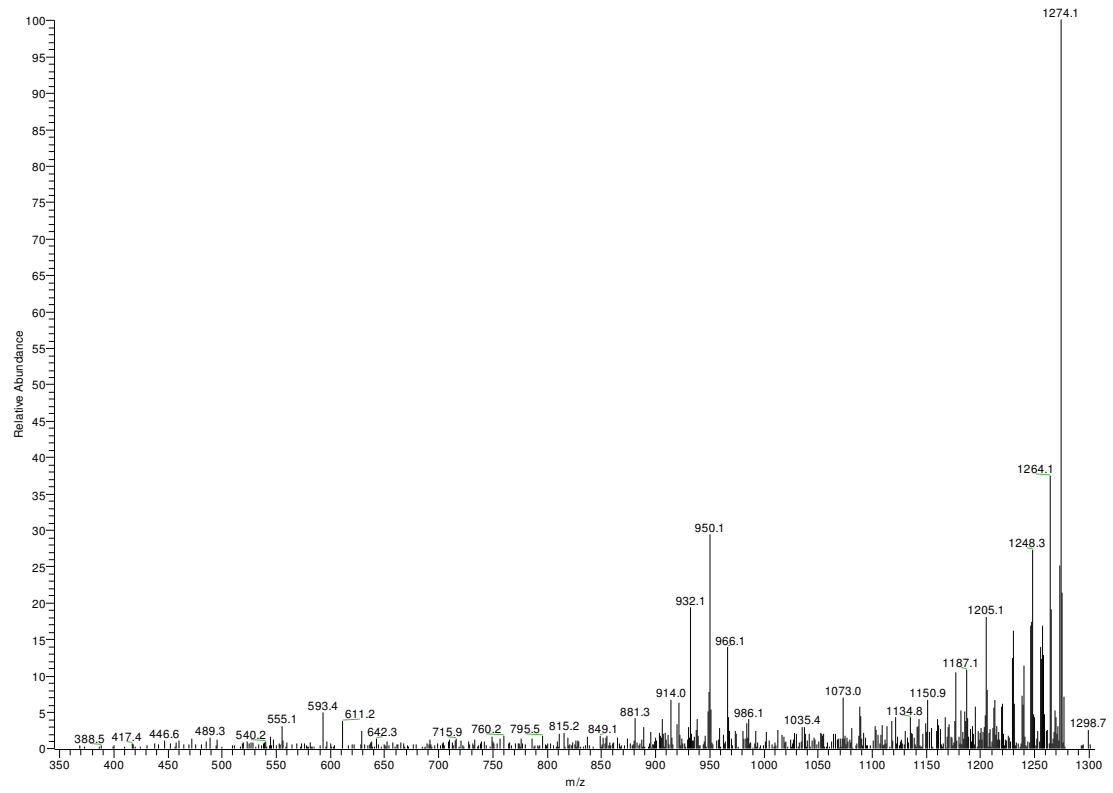
B

CID: 2ul #3324-3445 RT: 37.09-38.05 AV: 29 NL: 2.51E4
T: FTMS + p ESI Full ms [400.00-2000.00]



C

CID: 2ul #3319-5491 RT: 37.05-49.46 AV: 9 NL: 8.36E2
T: Average spectrum MS2 1292.16 (3319-5491)



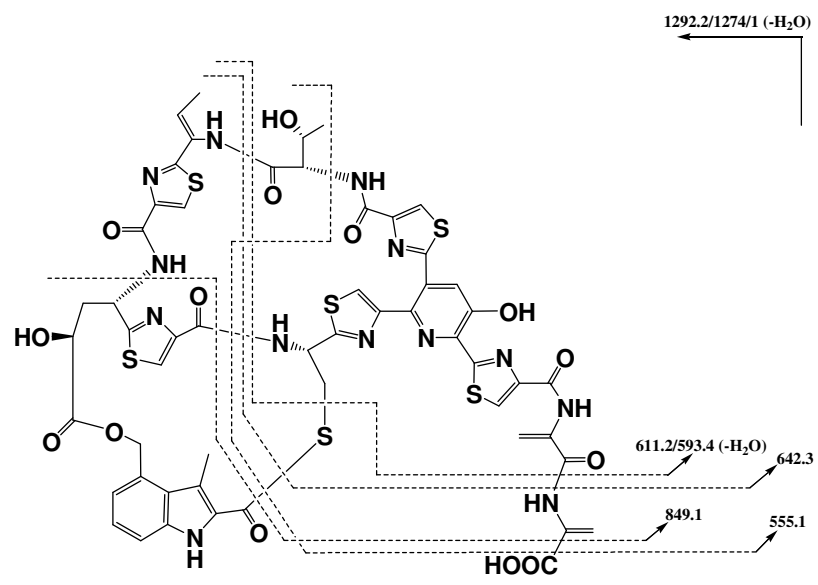
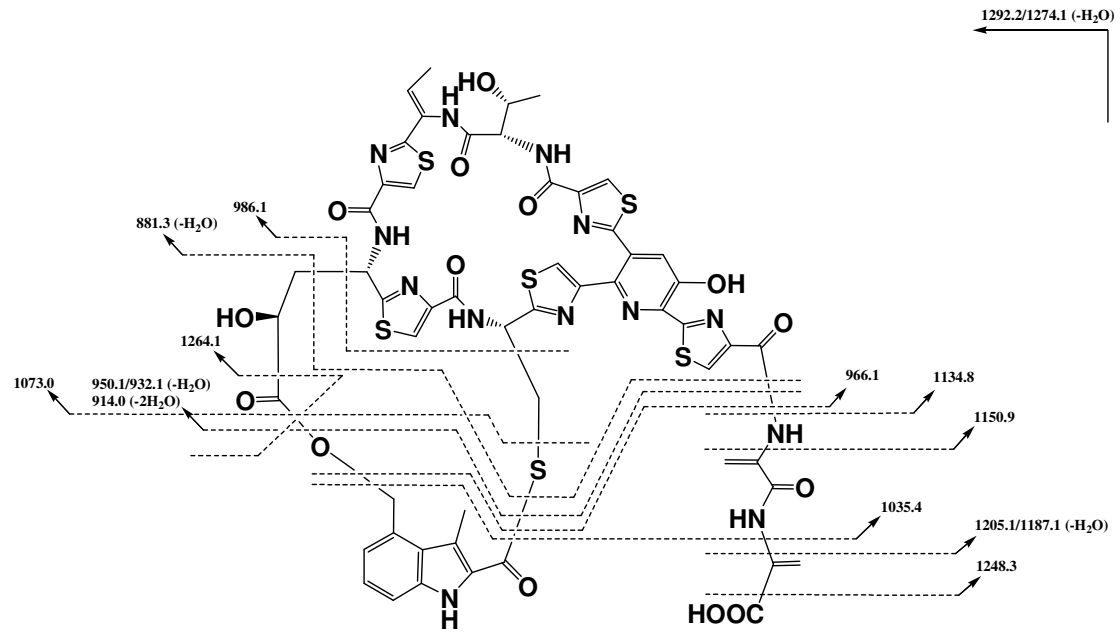
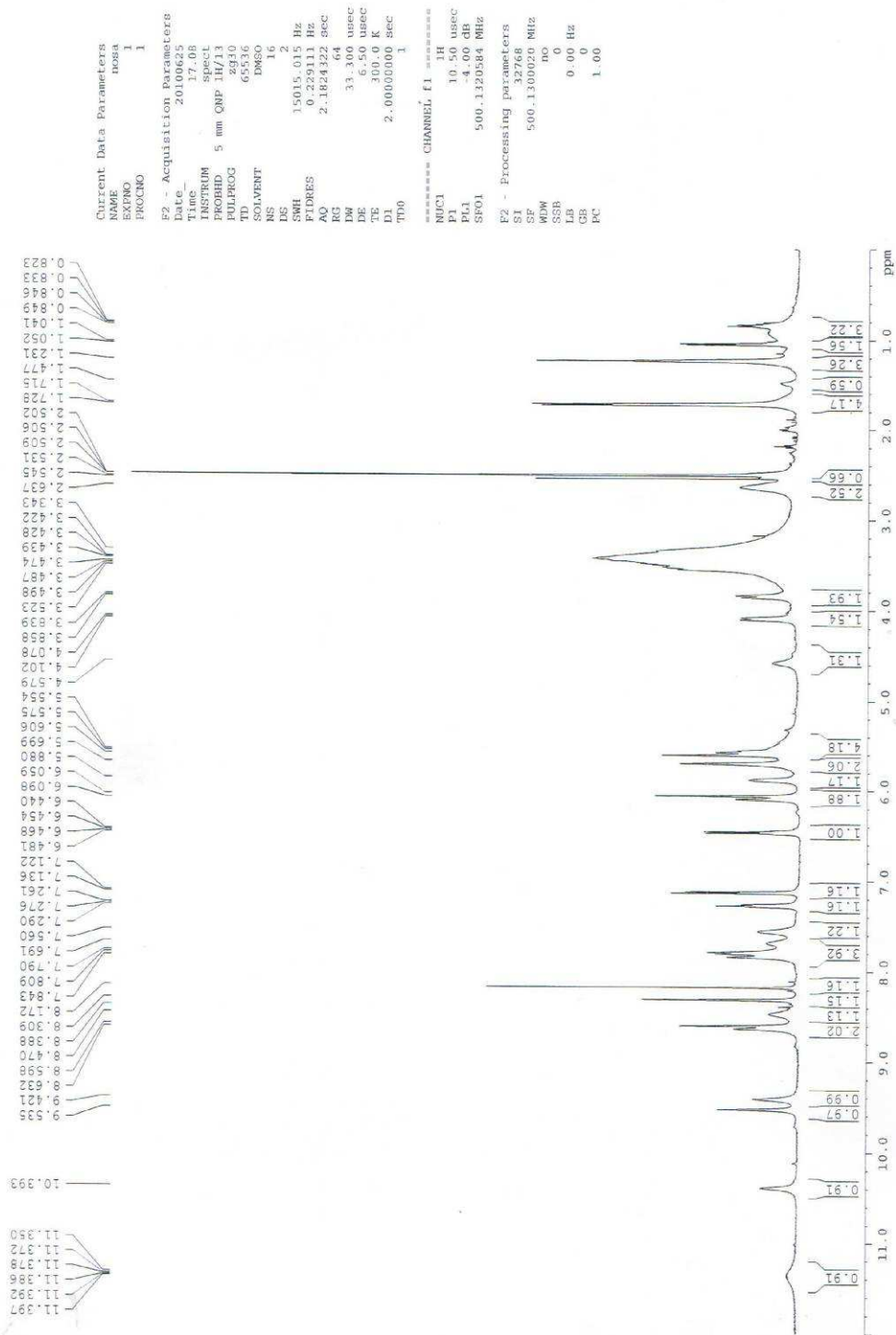
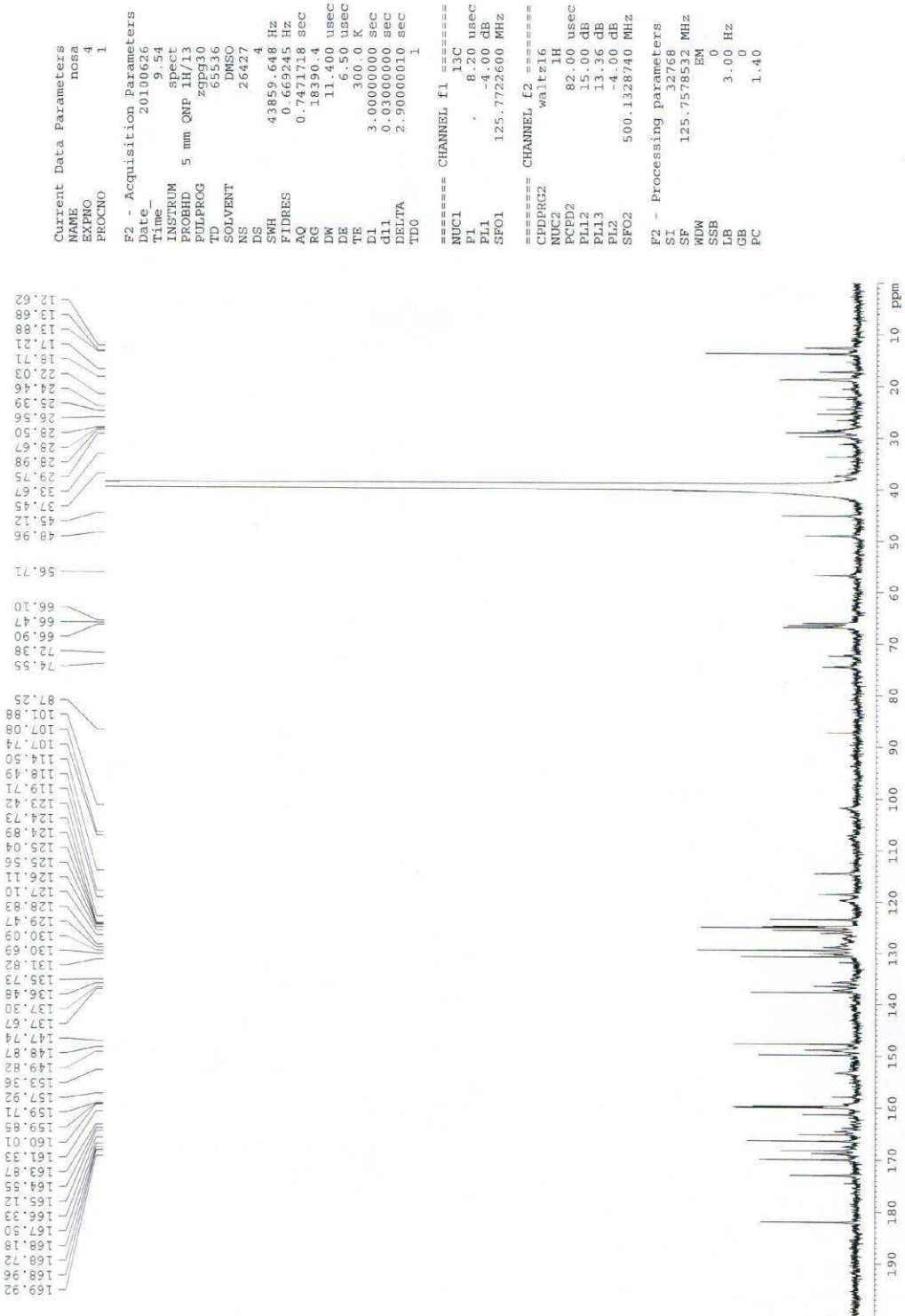


Figure S3. NMR spectra of the intermediate **2** for structural elucidation. A, ^1H NMR (500 MHz, d_6 -DMSO); B, ^{13}C NMR (125 MHz, d_6 -DMSO); C, HSQC; and D, HMBC.

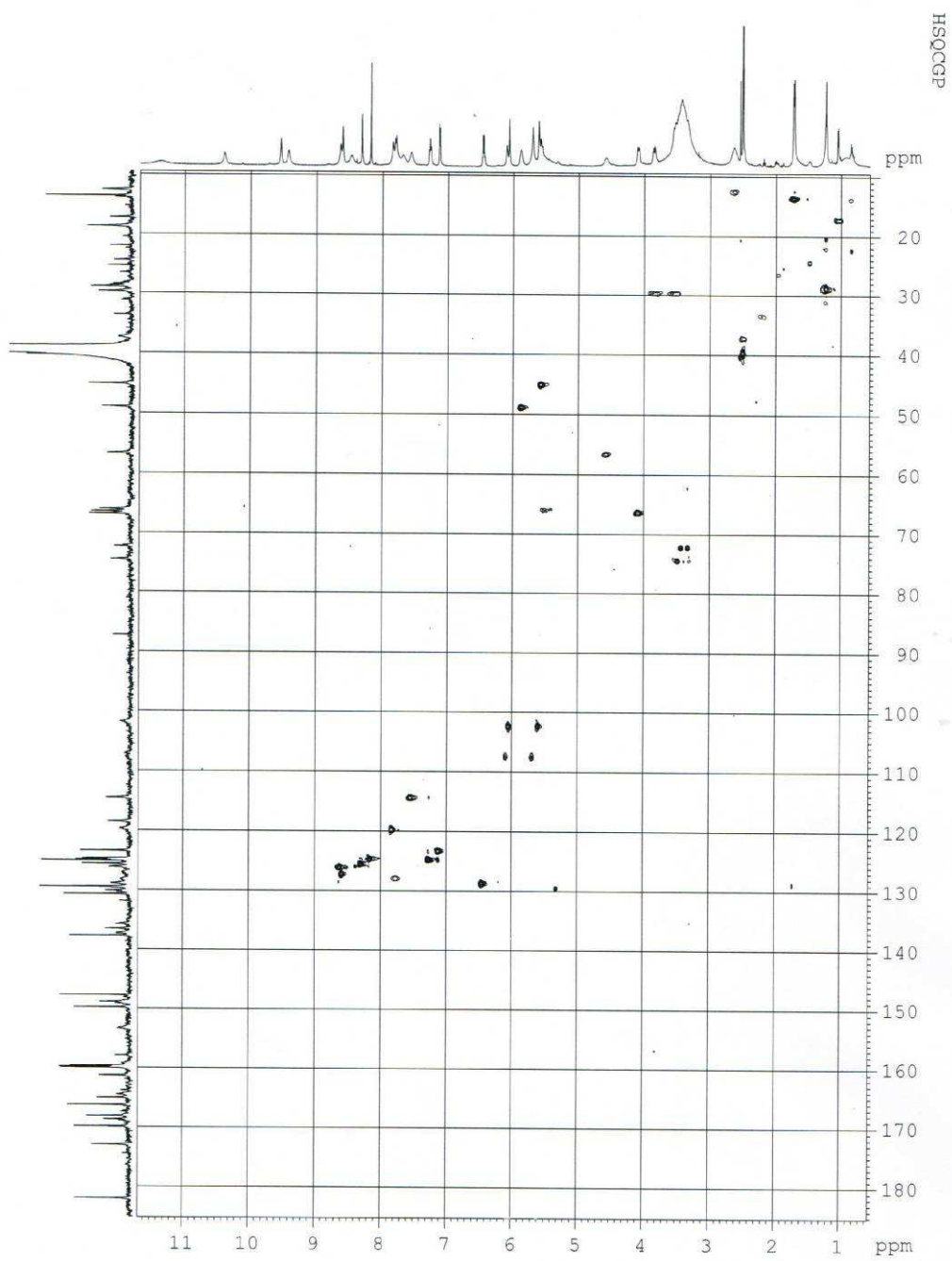
A



B



C



D

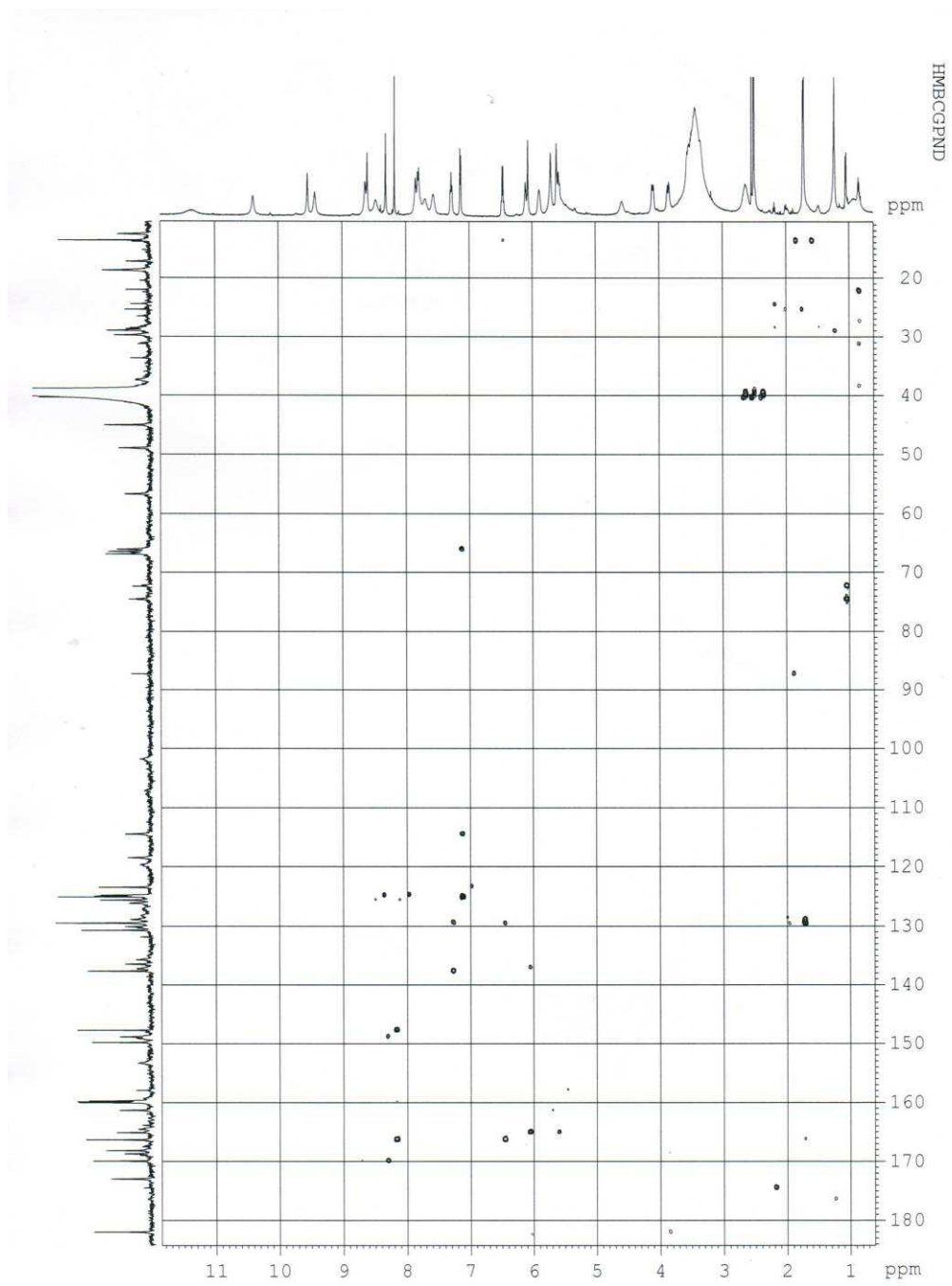


Figure S4. Sequence comparison of NosA in nosiheptide biosynthesis, NocA in nocathiacin biosynthesis, and TpdK in GE2270A biosynthesis.

```

NocA      -----VHLTIIWDLAESDQTVASLRSYLRDYAVEAYSATPGLRQKVVVANTGPEGE
NosA      MTEHPAQQLYCTVVLWDLRSAAATVASLRAYLRDHAVDAYTTVPGLRQKTWISSTGPEGE
TpdK      -----MYVVIVAFDLKESSVDFAE LR A WVRDRAADDYSRLPGMRFKTFWFSDE--RKR
           :: .:: :** .*  .*:**::** *.: *:  **:* *.*.:.  . .

NocA      TWGAVYLWDEKAAYGR---PPGVS RVV ELI GYAPTQRSYFSVEAGADGPLAGAL---AG
NosA      QWGAVYLWDSPEAAAYGR---PPGVS KV V ELI GYRPTERRYSVEAATEGPAAAAAPFGKG
TpdK      LWGAVYLVES-MLSFRDNLPLLPDGRTPVGVTRPTSMVLELEAFVTGPDGLD-----
           ***** :.  :.:*  *  .  .  :*  **  .: **  **  .

NocA      LGLAFTDPAAEPMRRPMEFNPPGASAFTLRADVVAGSPKQGGDGR
NosA      LGLAFDPASPELTRPQEFVPPGADAFIP-----SRPPA-----
TpdK      -----IEALARQGLSMTGGGHDH-----
           *.: *  . *  .

```

Figure S5. Structures of nosiheptide, nocathiacin I, GE2270A, thiostrepton, and siomycin A.

Dashed cycles indicate the terminal amide moiety.

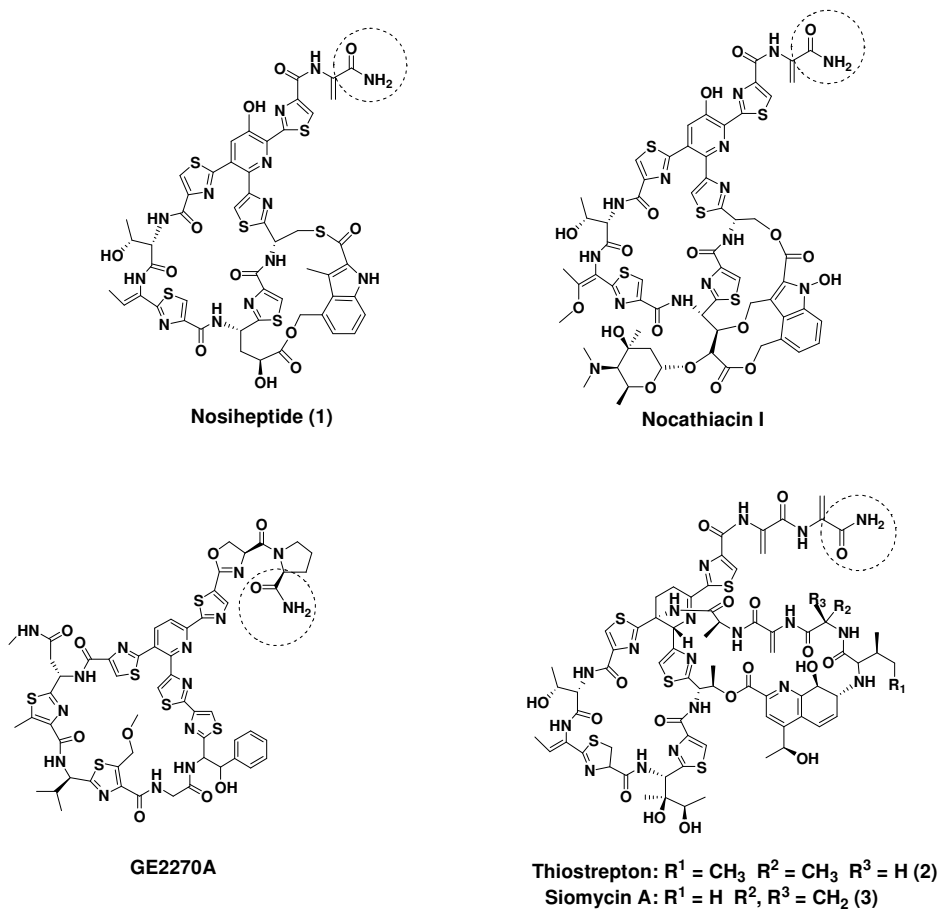
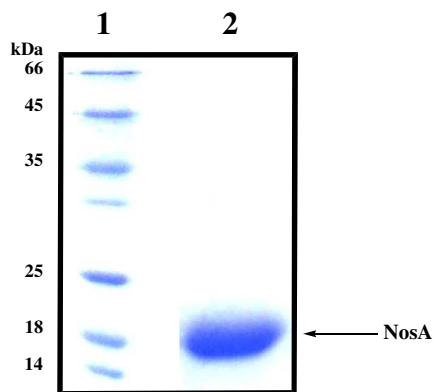


Figure S6. Analysis of the purified NosA. A, molecular mass marker (lane 1) and purified 6 x His-tagged NosA with the predicted molecular weight 18.3 kDa (lane 2) on a 12% sodium dodecyl sulfate-polyacrylamide gel; and B, its M^+ ion at $m/z = 18302.405$ shown by MALDI-TOF-MS analysis.

A



B

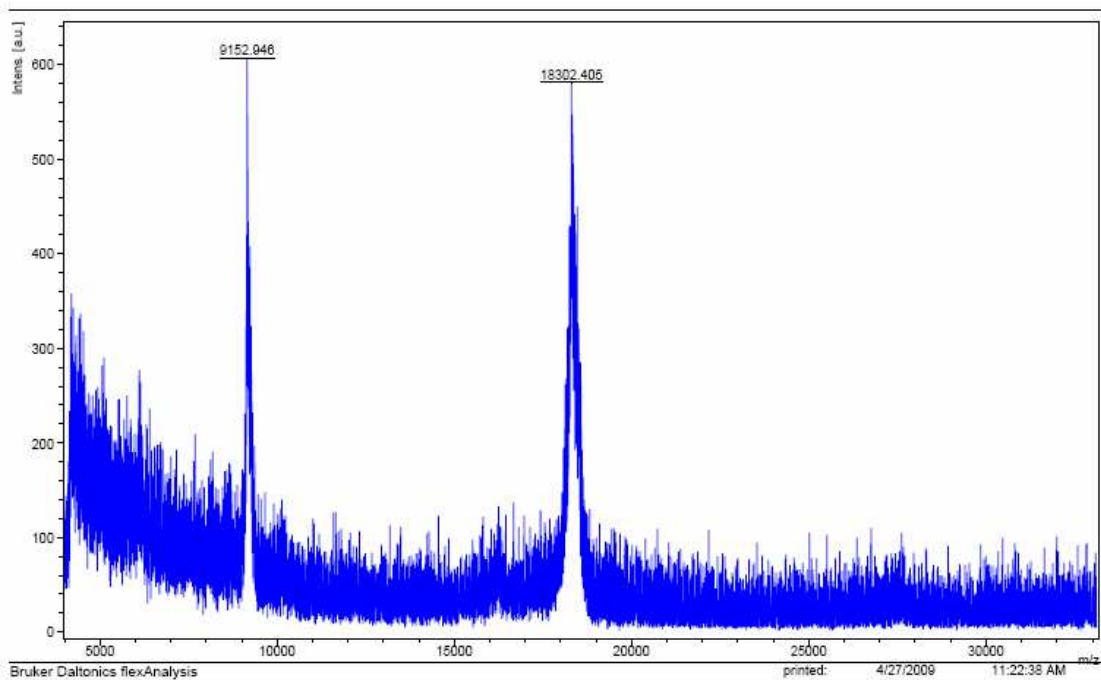
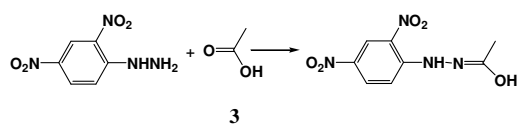


Figure S7. Identification of the co-product pyruvate (**3**) in NosA-catalyzed reaction. A, reaction of derivatization with 2,4-dinitrophenylhydrazine; B, probing of **3**, using 2,4-dinitrophenylhydrazine (**I**) and the corresponding derivative 2-(2,4-dinitrophenylhydrazono)-propanoic acid (**II**) as the controls, from the reactions catalyzed by NosA (**III**) and NosA inactivated by heating (**IV**), respectively.

A



B

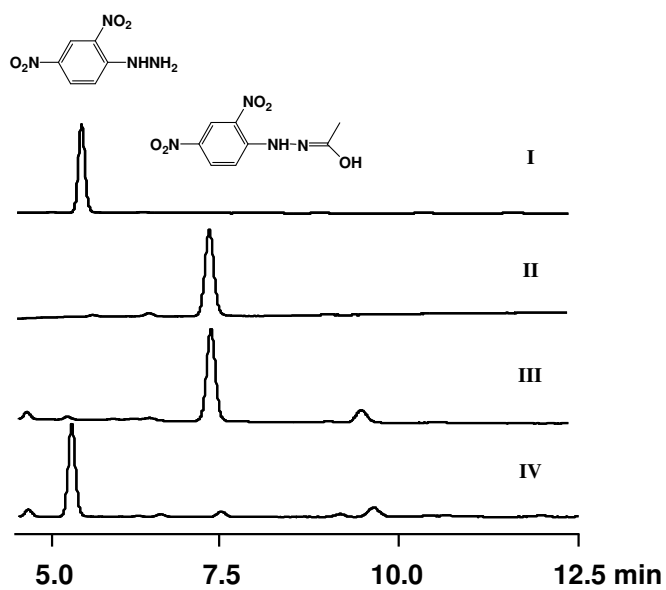


Figure S8. Effect of pH on the stability of the intermediate **2**. The solutions containing 60 μM **2** but varying in pH were incubated at 30°C for 17 hrs.

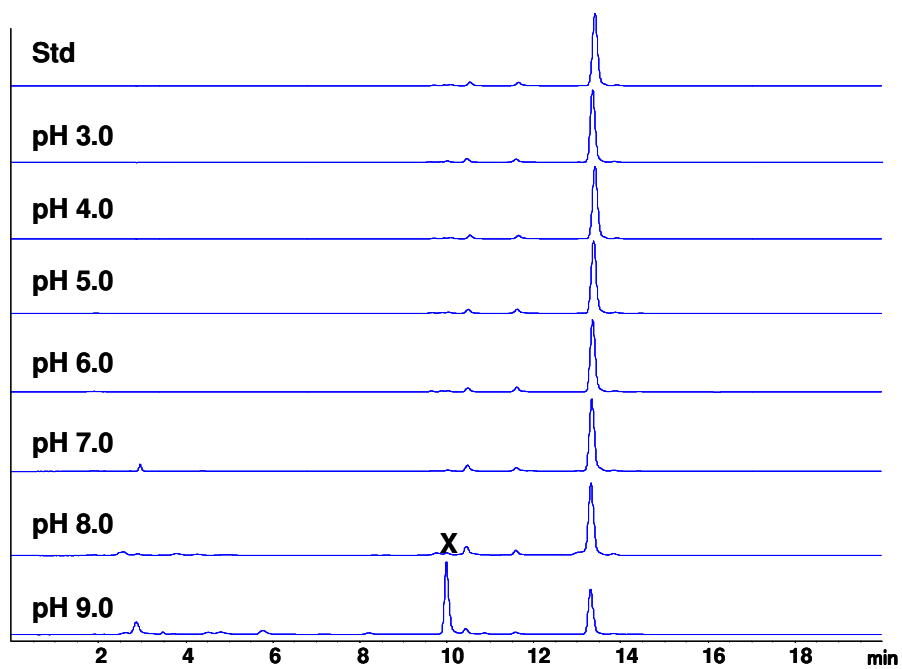


Figure S9. Time dependence for converting the intermediate **2** to the hydrolyzed product **X**. The solutions containing 60 μM **2** in 50 mM Tris-HCl (pH 9.0) buffer were incubated at 30°C, and then terminated by immediately storing at -80°C at 0 min, 30 min, 1 hr, 2 hr, 12 hr, and 17 hr, respectively, before product examination by HPLC-MS.

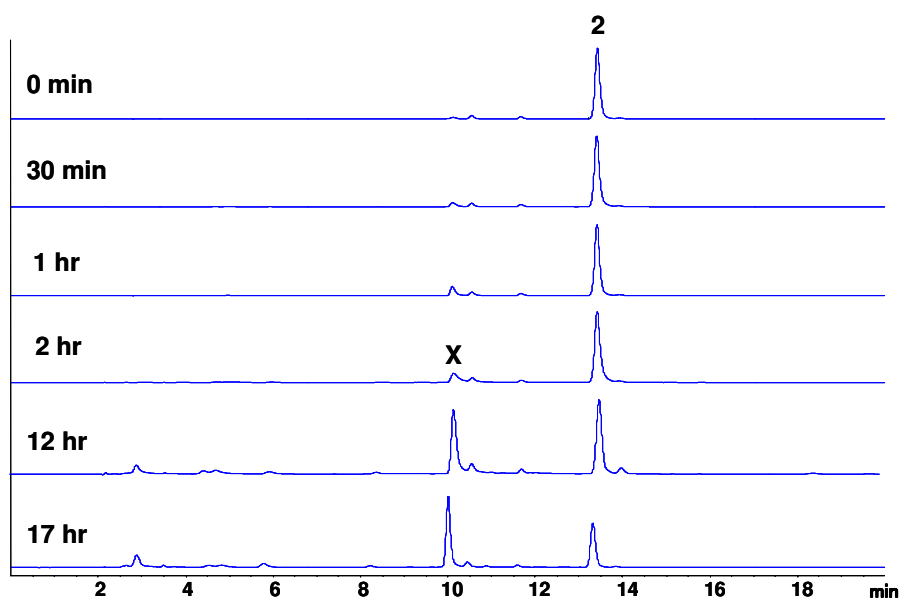
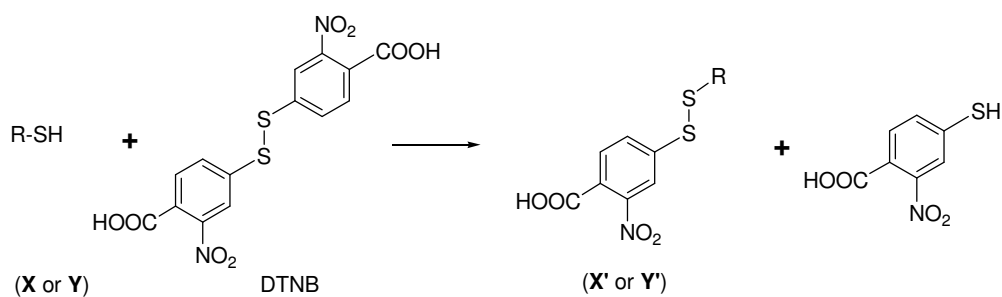


Figure S10. Sulfhydryl derivatization by adding of 5,5'-dithio-bis(2-nitrobenzoic acid) (DTNB). A, reaction of DTNB-based derivatization; and B, HPLC examination of converting **2** to **X** by incubation at pH 9.0 for 12 hrs in the absence of NosA (I), derivatization of **X** to its corresponding DTNB derivative **X'** (II), converting **X** to **Y** in the presence of NosA (III), and derivatization of **Y** to its corresponding DTNB derivative **Y'** (IV).

A



B

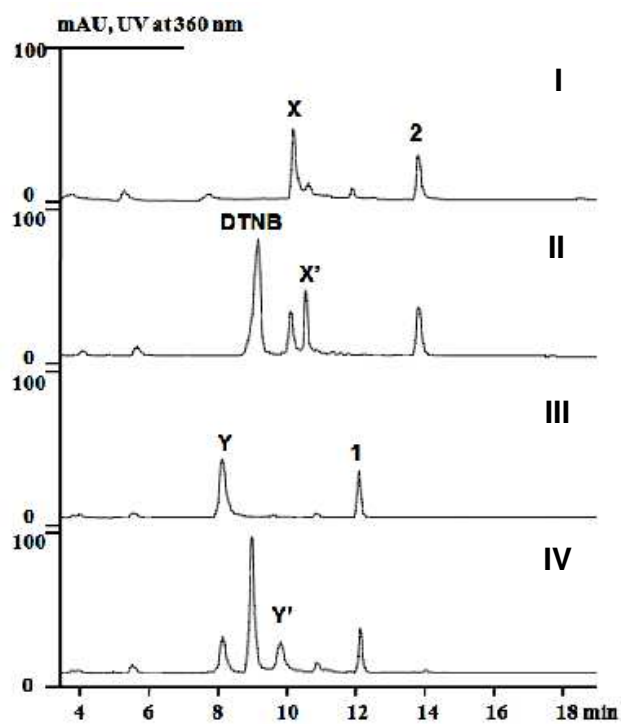
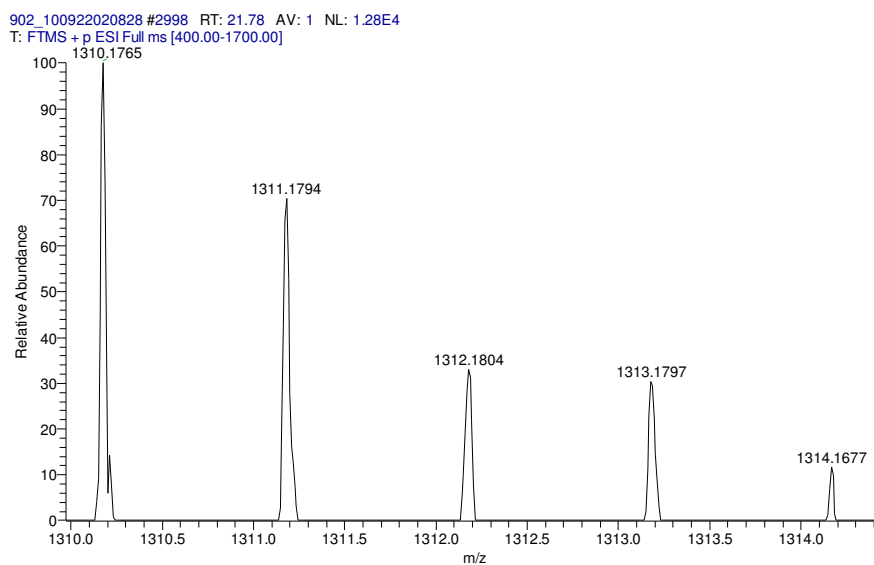


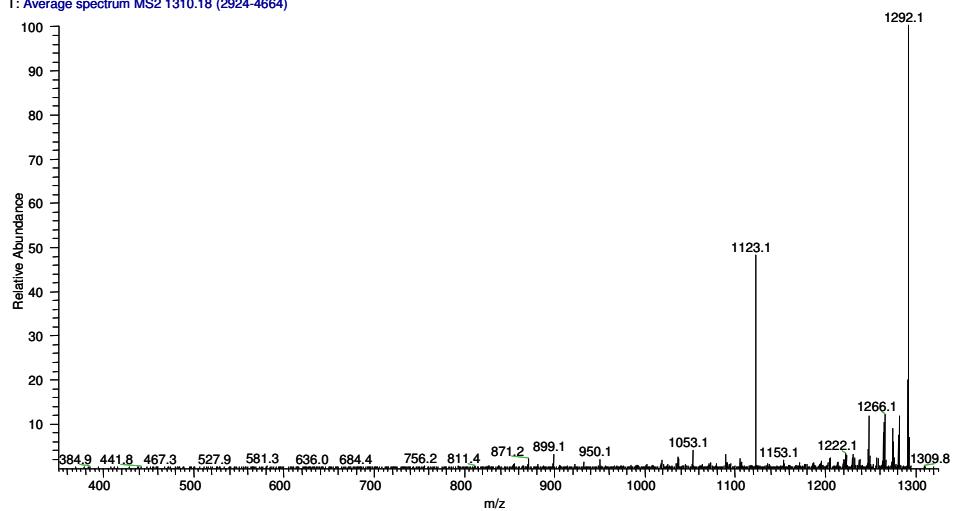
Figure S11. HR-ESI-MS and MS/MS analyses of compound **X** and its structural prediction. A, obtained profile for the $[M + H]^+$ ion of **X** by Orbitrap scanning; B, MS/MS analysis of the parent ion at $m/z = 1310.2$ corresponding to **X** by LTQ scanning and its fragments; and C, deduced structure of **X**.

A



B

902_100922020828 #2924-4664 RT: 21.30-32.50 AV: 38 NL: 7.74E2
T: Average spectrum MS2 1310.18 (2924-4664)



C

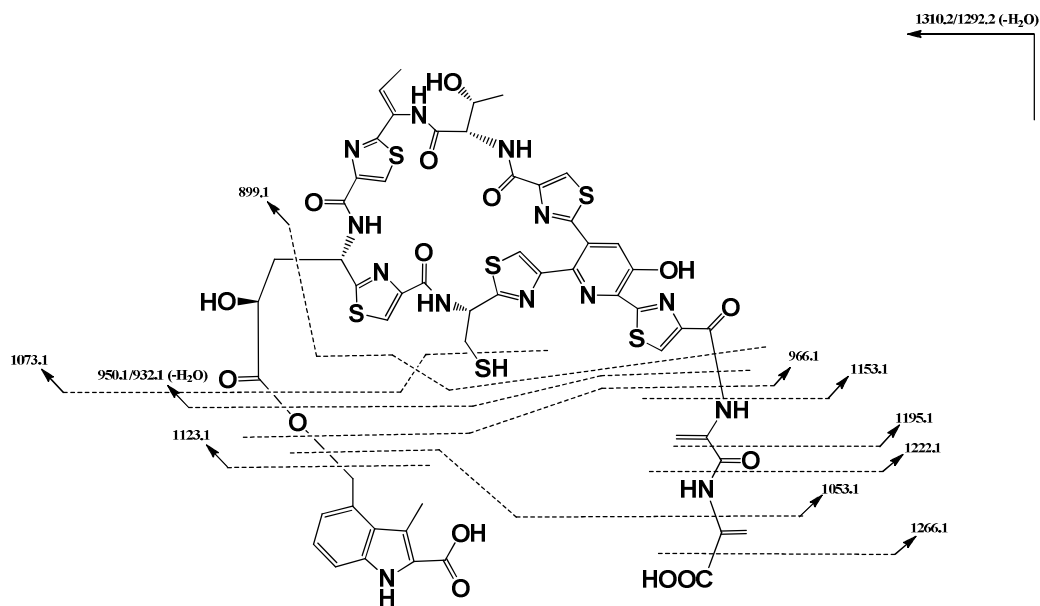
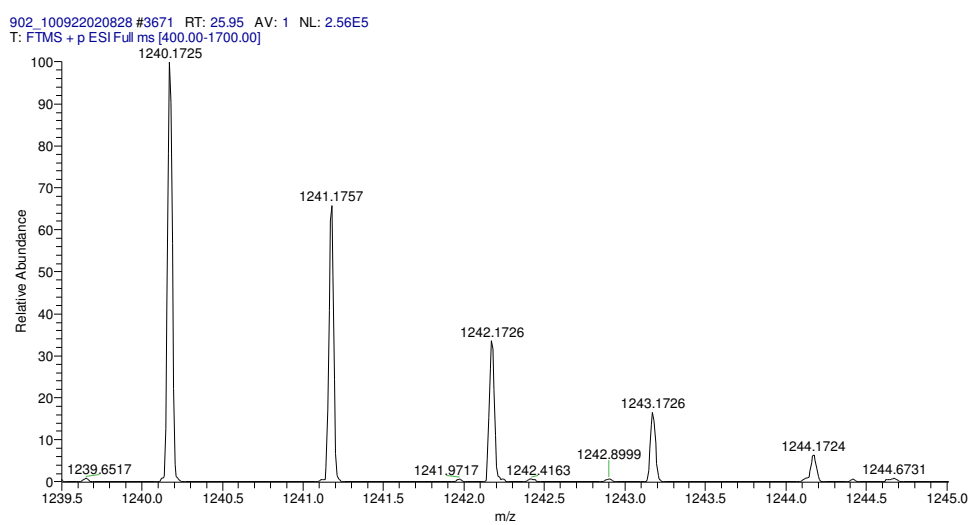
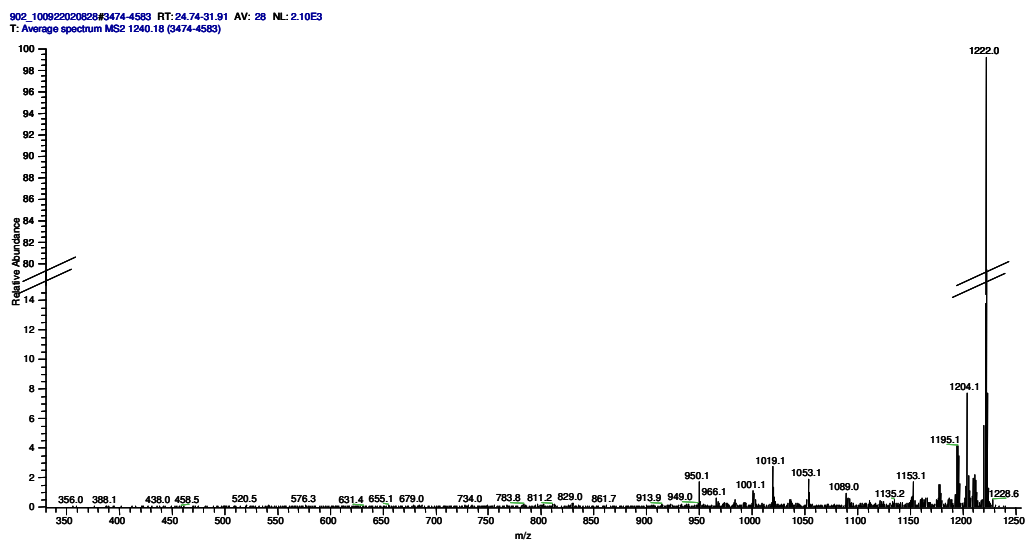


Figure S12. HR-ESI-MS and MS/MS analyses of compound **Y** and its structural prediction. A, obtained profile for the $[M + H]^+$ ion of **Y** by Orbitrap scanning; B, MS/MS analysis of the parent ion at $m/z = 1240.2$ corresponding to **Y** by LTQ scanning and its fragments; and C, deduced structure of **Y**.

A



B



C

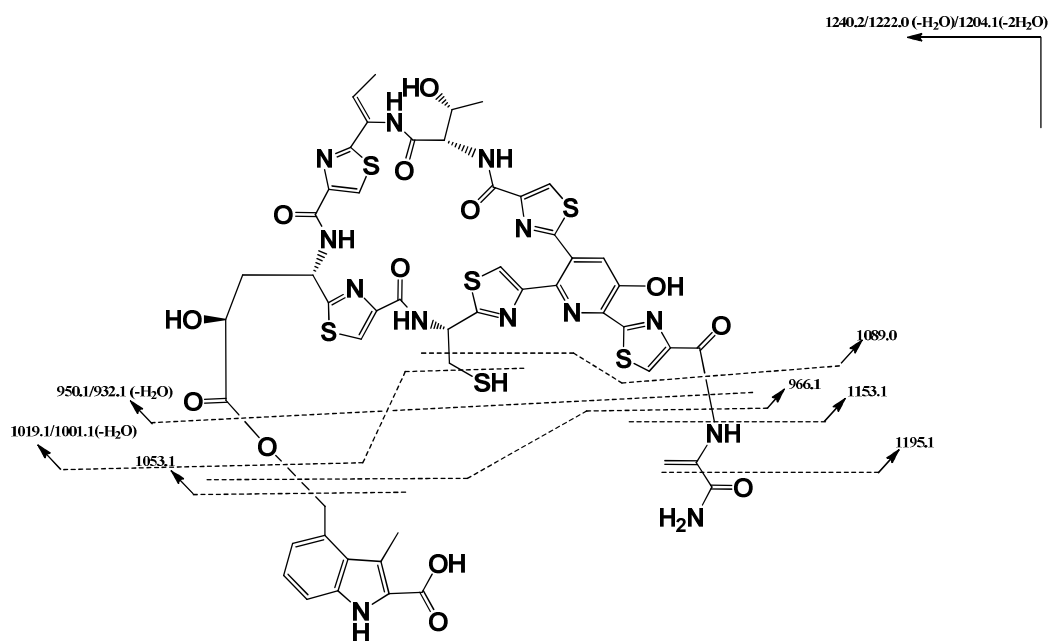


Figure S13. Effect of pH on the activity of NosA.

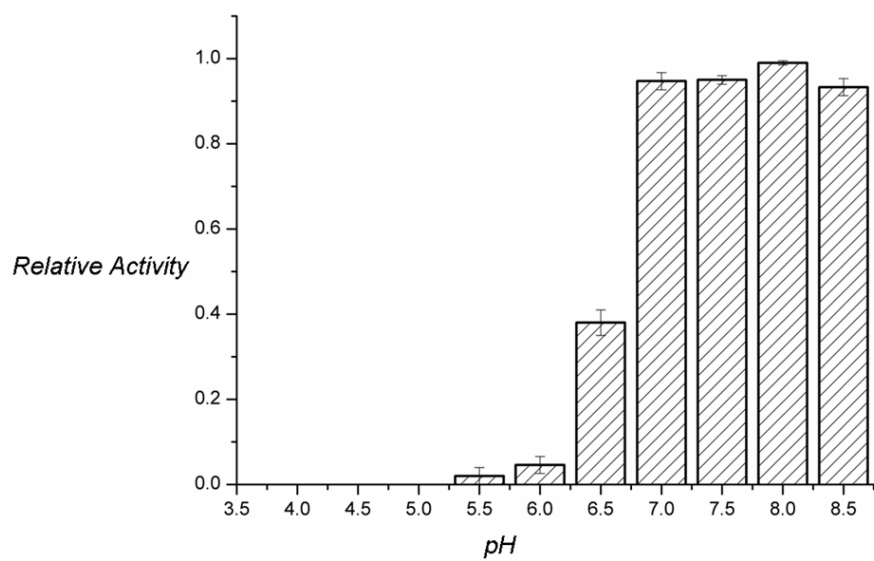
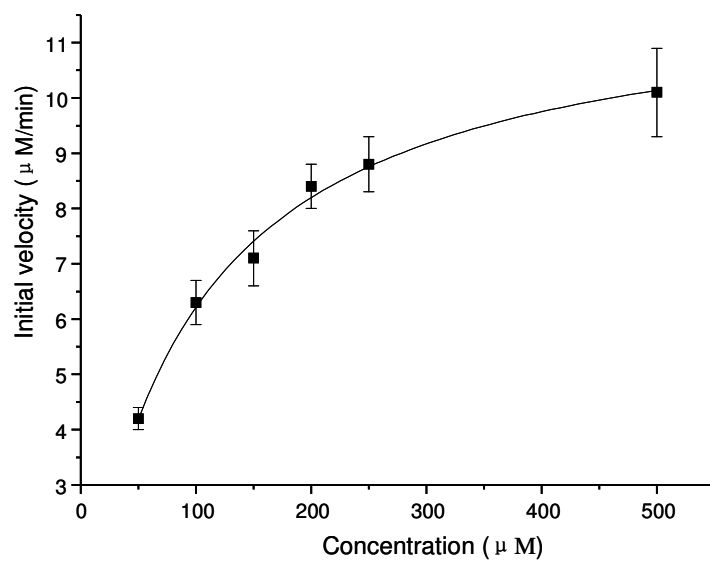


Figure S14. Kinetic characterization of NosA by plotting the initial velocities of **1** production.



References

- (1) Kieser, T.; Bibb, M.; Butter, M.; Chater, K. F.; Hopwood, D. A. *Practical Streptomyces Genetics*, The John Innes Foundation, Norwich, **2001**.
- (2) Sambrook, J.; Russell, D. W. *Molecular Cloning: A Laboratory Manual*, 3rd ed., Cold Spring Harbor Laboratory Press, New York, **2001**.
- (3) Yu, Y.; Duan, L.; Zhang, Q.; Liao, R.; Ding, Y.; Pan, H.; Wendt-Pienkowski, E.; Tang, G.; Shen, B.; Liu, W. *ACS Chem. Biol.* **2009**, 4, 855-864.
- (4) Ding, Y.; Yu, Y.; Pan, H.; Guo, H.; Li, Y.; Liu, W. *Mol. BioSyst.* **2010**, 6, 1180-1185.
- (5) Liao, R.; Duan, L.; Lei, C.; Pan, H.; Ding, Y.; Zhang, Q.; Chen, D.; Shen, B.; Yu, Y.; Liu, W. *Chem. Biol.* **2009**, 16, 141-147.
- (6) MacNeil, D. J.; Gewain, K. M.; Ruby, C. L.; Dezeny, G.; Gibbons, P. H.; MacNeil, T. *Gene* **1992**, 111, 61-68.
- (7) Bierman, M.; Logan, R.; O'Brien, K.; Seno, E. T.; Rao, R. N.; Schoner, B. E. *Gene* **1992**, 116, 44-49.
- (8) Pucci, M. J.; Bronson, J. J. ; Barrett, J. F. ; DenBleyker, K. L.; Discotto, L. F.; Fung-Tomc, J. C.; Ueda, Y. *Antimicrob. Agents. Chemother.* **2004**, 48, 3697-3701.
- (9) McFarland, J. *J. Am. Med. Assoc.* **1907**, 49, 1176-1178.